

A fully quantal molecular description for the spectra of bosons and fermions in the lowest Landau level

Constantine Yannouleas and Uzi Landman

School of Physics, Georgia Institute of Technology, Atlanta, Georgia 30332-0430

(Dated: 19 February 2010; An extended version was published as Phys. Rev. A **81**, 023609 (2010); see arXiv:1001.1090)

Through the introduction of a class of appropriate translationally invariant trial wave functions, we show that the strong correlations in the lowest Landau level (LLL) reflect in finite systems the emergence of intrinsic point-group symmetries associated with rotations and vibrations of molecules formed through particle localization. This quantal molecular description is universal, being valid for both bosons and fermions, for both the yrast and excited states of the LLL spectra, and for both low and high angular momenta. "Quantum-fluid" physical pictures associated with Jastrow-type trial functions are shown to be reducible to the molecular description introduced in this paper.

PACS numbers: 03.75.Hh, 03.75.Lm, 73.43.-f, 73.21.La

Motivation. – Following the discovery [1] of the fractional quantum Hall effect (FQHE) in two-dimensional (2D) semiconductor heterostructures under high magnetic fields (B), the description of strongly correlated electrons in the lowest Landau level (LLL) developed into a major branch of theoretical condensed matter physics [2–10].

Most recently, the burgeoning fields of semiconductor [9] quantum dots and rapidly rotating trapped ultracold neutral gases [11–22] have generated significant interest pertaining strongly correlated states in the lowest Landau level. Furthermore, it is anticipated that small (and/or mesoscopic) assemblies of ultracold bosonic atoms will become technically available in the near future [20, 21] and that they will provide an excellent vehicle [15, 16, 19–22] for experimentally reaching exotic phases and for testing the rich variety of proposed LLL trial wave functions, including the Jastrow-Laughlin (JL) [2], composite-fermion (CF) [7], Moore-Read [4], and rotating Wigner molecule (REM) [8, 9] trial functions.

A universal physical description of the full LLL spectra (including both yrast [23] and all excited states), however, is still missing. To remedy this, a unified theory for the LLL spectra of a small number of particles valid for both statistics (i.e., for both bosons and fermions) is introduced in this paper. The LLL spectra are shown to be associated with *fully quantal* [24] and strongly correlated ro-vibrational molecular (RVM) states, i.e., with (analytic) trial functions describing vibrational excitations relative to the set of special yrast states that exhibit enhanced stability and magic angular momenta, and are referred to as cusp states. The cusp states, important as they are, represent only a small fraction of the LLL spectrum. The molecular trial functions associated with them are purely rotational (i.e., vibrationless) and were introduced for the case of electrons in Ref. [8] under the name rotating electron molecules (REMs). The corresponding *analytic* bosonic trial functions for cusp states [called rotating boson molecules (RBMs)] are introduced in this paper; see Eq. (3).

It is remarkable that the numerical results of the present theory were found in all tested cases to agree within machine precision with exact-diagonalization (EXD) results, including energies, wave functions, and overlaps. This numerical behavior points toward a deeper mathematical finding, i.e., that the RVM trial functions for both statistics provide a *correlated* basis (see below) that spans the translationally invariant (TI) subspace [3] of the LLL spectrum. An uncorrelated basis, without physical meaning, built out of products of elementary symmetric polynomials is also known to span the (bosonic) TI subspace [25]. We are, however, unaware of any other correlated functions which span this subspace. Indeed, although the Jastrow-Laughlin function is translationally invariant, its quasi-hole and quasi-electron excitations are not [3]. Similarly, the compact composite-fermion trial functions are translationally invariant [18], but the CF excitations which are needed to complete the CF basis are not [10]. The shortcoming of the above well known correlated LLL theories to satisfy fundamental symmetries of the many-body Hamiltonian represents an unsatisfactory state of affairs, and the present paper provides a remedy to this effect. At the same time a different physical picture is being established: that is, the RVM functions and corresponding molecular point-group symmetries are superior in expressing and interpreting the emergent many-body correlations of the LLL states.

Theory. – The RVM functions have the general form (within a normalization constant):

$$\Phi_{\mathcal{L}}^{\text{RXM}}(n_1, n_2) Q_{\chi}^m |0\rangle, \quad (1)$$

where (n_1, n_2) indicates the molecular configuration (here we consider two concentric rings) of point-like particles with n_1 (n_2) particles in the first (second) ring. The particles on each ring form regular polygons. The index RXM stands for either REM, i.e., a rotating electron molecule, or RBM, i.e., a rotating boson molecule. $\Phi_{\mathcal{L}}^{\text{RXM}}(n_1, n_2)$ alone describes pure molecular rotations associated with magic angular momenta $\mathcal{L} = \mathcal{L}_0 + n_1 k_1 + n_2 k_2$, with k_1, k_2 being nonnegative

integers; $\mathcal{L}_0 = N(N-1)/2$ for electrons and $\mathcal{L}_0 = 0$ for bosons. The product in Eq. (1) combines rotations with vibrational excitations, the latter being denoted by Q_λ^m , with λ being an angular momentum; the superscript denotes raising to a power m . Both $\Phi_{\mathcal{L}}^{\text{RXM}}$ and Q_λ^m are homogeneous polynomials of the complex particle coordinates z_1, z_2, \dots, z_N , of order \mathcal{L} and λm , respectively. The total angular momentum $L = \mathcal{L} + \lambda m$. Q_λ^m is always symmetric in these variables; $\Phi_{\mathcal{L}}^{\text{RXM}}$ is antisymmetric (symmetric) for fermions (bosons). $|0\rangle = \prod_{i=1}^N \exp[-z_i z_i^*/2]$; this product of Gaussians will be omitted henceforth.

The analytic expressions for the $\Phi_{\mathcal{L}}^{\text{REM}}$ (for fully polarized electrons) were derived in Ref. [8] employing a two-step method: (i) First a single Slater *determinant* [that breaks the rotational (circular) symmetry] was constructed using displaced Gaussians as electronic orbitals, i.e.,

$$u(z, Z_j) = \frac{1}{\sqrt{\pi}} \exp[-|z - Z_j|^2/2] \exp[-i(xY_j + yX_j)]. \quad (2)$$

The phase factor is due to the gauge invariance. $z \equiv x - iy$, and all lengths are in dimensionless units of $l_B\sqrt{2}$, with the magnetic length $l_B = \sqrt{\hbar/(m_e\omega_c)}$; $\omega_c = eB/(m_e c)$ is the cyclotron frequency. The centers $Z_j \equiv X_j + iY_j$, $j = 1, 2, \dots, N$ of the Gaussians are the vertices of the regular polygons in the (n_1, n_2) geometric arrangement. (ii) A subsequent step of symmetry restoration was performed using the projection operator $\mathcal{P}(\mathcal{L}) = \frac{1}{2\pi} \int_0^{2\pi} d\gamma e^{i\gamma(\hat{L} - \mathcal{L})}$, where $\hat{L} = \sum_{i=1}^N \hat{l}_i$ is the total angular momentum operator; this yielded trial wave functions with good total angular momenta \mathcal{L} [8, 9].

Analytic expressions for the $\Phi_{\mathcal{L}}^{\text{RBM}}$ (for spinless bosons) can also be derived using the two-step method. Naturally, in the first step one constructs a *permanent* out of the orbitals of Eq. (2); one also uses the equivalence $\omega_c \rightarrow 2\Omega$ between the cyclotron frequency ω_c (electrons) and the rotational frequency Ω (bosons) [9]. Here we present as an illustrative example the simpler case of $N = 3$ (and $N = 4$ in the Appendix) bosons having a $(0, N)$ one-ring molecular configuration. One has (within a normalization constant)

$$\Phi_{\mathcal{L}}^{\text{RBM}}(0, 3) = \sum_{0 \leq l_1 \leq l_2 \leq l_3}^{l_1 + l_2 + l_3 = \mathcal{L}} C(l_1, l_2, l_3) \text{Perm}[z_1^{l_1}, z_2^{l_2}, z_3^{l_3}], \quad (3)$$

where the symbol "Perm" denotes a permanent with elements $z_i^{l_j}$, $i, j = 1, 2, 3$; only the diagonal elements are shown in Eq. (3). The coefficients were found to be:

$$C(l_1, l_2, l_3) = \left(\prod_{i=1}^3 l_i! \right)^{-1} \left(\prod_{k=1}^M p_k! \right)^{-1} \times \left(\sum_{1 \leq i < j \leq 3} \cos \left[\frac{2\pi(l_i - l_j)}{3} \right] \right), \quad (4)$$

where $1 \leq M \leq 3$ denotes the number of different indices in the triad (l_1, l_2, l_3) and the p_k 's are the multiplicities of each one of the different indices. For example, for $(1, 1, 4)$, one has $M = 2$ and $p_1 = 2, p_2 = 1$.

The $\Phi_{\mathcal{L}}^{\text{REM}}$ expressions for electrons in a $(0, N)$ or a $(1, N-1)$ configuration are given by Eqs. (6.2) and (6.4) of Ref. [9], respectively. For electrons (1) $M = N$ in all instances and (2) a *product of sine* terms replaces the *sum of cosine* terms appearing in Eq. (4).

We note that $\Phi_{\mathcal{L}}^{\text{RXM}}(n_1, n_2) = 0$ for both bosons and electrons when $\mathcal{L} \neq \mathcal{L}_0 + n_1 k_1 + n_2 k_2$. This selection rule follows directly from the point group symmetries of the (n_1, n_2) molecular configurations.

The vibrational excitations Q_λ are given by the same expression for both bosons and electrons, namely, by the symmetric polynomials:

$$Q_\lambda = \sum_{i=1}^N (z_i - z_c)^\lambda, \quad (5)$$

where $z_c = (1/N) \sum_{i=1}^N z_i$ is the coordinate of the center of mass and $\lambda > 1$ is a prime number. Vibrational excitations of a similar form, i.e., $\tilde{Q}_\lambda = \sum_{i=1}^N z_i^\lambda$ (and certain other variations), have been used earlier to approximate *part* of the LLL spectra. Such earlier endeavors provided valuable insights, but overall they remained inconclusive; e.g., for electrons in the neighborhood of the maximum density droplet [with fractional filling $\nu = 1$ ($\nu = N(N-1)/2\mathcal{L}$)], see Refs. [5] and [6], and for bosons in the range $0 \leq L \leq N$, see Refs. [11, 13, 14].

The advantage of Q_λ is that it is translationally invariant (TI) [3, 13], a property shared with both $\Phi_{\mathcal{L}}^{\text{RBM}}$ and $\Phi_{\mathcal{L}}^{\text{REM}}$. In the following, we will discuss illustrative cases, which will show that the RVM functions of Eq. (1) provide a correlated basis (RVM basis) that spans the TI subspace [3, 13, 18] of *nonspurious* states in the LLL spectra. The dimension $D^{\text{TI}}(L)$ of the RVM-diagonalization space (using the RVM basis) is much smaller than the dimension $D^{\text{EXD}}(L)$ of the exact-diagonalization (EXD) [9] space spanned by uncorrelated determinants $\text{Det}[z_1^{l_1}, \dots, z_N^{l_N}]$ or permanents $\text{Perm}[z_1^{l_1}, \dots, z_N^{l_N}]$ formed with Darwin-Fock orbitals. The remaining $D^{\text{EXD}}(L) - D^{\text{TI}}(L)$ states are *spurious* center-of-mass excitations (generated by applying \tilde{Q}_1^m) whose energies coincide with those appearing at all the other smaller angular momenta [3]. Thus $D^{\text{TI}}(L) = D^{\text{EXD}}(L) - D^{\text{EXD}}(L-1)$; see TABLE I.

Three spinless bosons – Only the $(0, 3)$ molecular configuration and the dipolar $\lambda = 2$ vibrations are at play (as checked numerically), i.e., the full TI spectra at any L are spanned by the wave functions

$$\Phi_{3k}^{\text{RBM}}(0, 3) Q_2^m \Rightarrow \{k, m\}, \quad (6)$$

with $k, m = 0, 1, 2, \dots$, and $L = 3k + 2m$; these states are always orthogonal. This represents a remarkable analogy with the case of $N = 3$ electrons (see below).

TABLE I: LLL spectra of three spinless bosons interacting via a repulsive contact interaction $g\delta(z_i - z_j)$. 2nd column: Dimensions of the EXD and the nonspurious TI (in parenthesis) spaces (the EXD space is spanned by uncorrelated permanents of Darwin-Fock orbitals). 4th to 6th columns: Matrix elements [in units of $g/(\pi\Lambda^2)$, $\Lambda = \sqrt{\hbar/(m\Omega)}$] of the contact interaction between the correlated RVM states $\{k, m\}$ [see Eq. (6)]. The total angular momentum $L = 3k + 2m$. Last three columns: Energy eigenvalues from the RVM diagonalization of the associated matrix of dimension $D^{\text{TI}}(L)$. There is no nonspurious state with $L = 1$. The full EXD spectrum at a given L is constructed by including, in addition to the listed TI eigenvalues [$D^{\text{TI}}(L)$ in number], all the energies associated with angular momenta smaller than L . An integer in square brackets indicates the energy ordering in the full EXD spectrum (including both spurious and TI states). Seven decimal digits are displayed, but the energy eigenvalues from the RVM diagonalization agree with the corresponding EXD-TI ones within machine precision.

L	$D^{\text{EXD}}(D^{\text{TI}})$	$\{k, m\}$	Matrix elements			Energy eigenvalues (RVM diag. or EXD-TI)		
0	1(1)	{0,0}	1.5000000			1.5000000[1]		
2	2(1)	{0,1}	0.7500000			0.7500000[1]		
3	3(1)	{1,0}	0.3750000			0.3750000[1]		
4	4(1)	{0,2}	0.5625000			0.5625000[2]		
5	5(1)	{1,1}	0.4687500			0.4687500[2]		
6	7(2)	{2,0}	0.0468750	0.1482318				
		{0,3}	0.1482318	0.4687500		0.0000000[1]	0.5156250[4]	
7	8(1)	{1,2}	0.4921875			0.4921875[4]		
8	10(2)	{2,1}	0.0937500					
		{0,4}	0.1960922	0.4101562		0.0000000	0.5039062[6]	
12	19(3)	{4,0}	7.3242187×10^{-4}	1.0863572×10^{-2}	1.5742811×10^{-2}			
		{2,3}	1.0863572×10^{-2}	0.1611328	0.2335036			
		{0,6}	1.5742811×10^{-2}	0.2335036	0.3383789	0.0000000	0.0000000	0.5002441[13]

TABLE I provides the systematics of the molecular description for the beginning ($0 \leq L \leq 12$) of the LLL spectrum. There are several cases when the TI subspace has dimension one and the exact solution coincides with a single $\{k, m\}$ state. For $L = 0$ the exact solution coincides with $\Phi_0^{\text{RBM}} = 1$ ($Q_\lambda^0 = 1$); this is the only case when an LLL state has a Gross-Pitaevskii form, i.e., it is a single permanent [see $|0\rangle$ in Eq. (1)]. For $L = 2$, we found $\Phi_{[1]}^{\text{exact}} \propto Q_2$ (for the index $[i]$, see caption of TABLE I), and since [see Eq. (5)] $Q_2 \propto (z_1 - z_c)(z_2 - z_c) + (z_1 - z_c)(z_3 - z_c) + (z_2 - z_c)(z_3 - z_c)$, this result agrees with the findings of Refs. [13, 26] concerning ground states of bosons in the range $0 \leq L \leq N$. For $L = 3$, one finds $\Phi_{[1]}^{\text{exact}} \propto \Phi_3^{\text{RBM}}$. Since $\Phi_3^{\text{RBM}} \propto (z_1 - z_c)(z_2 - z_c)(z_3 - z_c)$ [see Eq. (3)], this result agrees again with the findings of Refs. [13, 26]. For $L = 5$, the single non-spurious state is an excited one, $\Phi_{[2]}^{\text{exact}} \propto \Phi_3^{\text{RBM}} Q_2$. For $L = 6$, the ground-state is found to be $\Phi_{[1]}^{\text{exact}} \propto -160\Phi_6^{\text{RBM}}/9 + Q_2^3/4 = (z_1 - z_2)^2(z_1 - z_3)^2(z_2 - z_3)^2$, i.e., the bosonic Laughlin function for $\nu = 1/2$ is equivalent to an RBM state that incorporates vibrational correlations. For $L \geq N(N - 1)$ (i.e., $\nu \leq 1/2$), the EXD yrast energies equal zero, and with increasing L the degeneracy of the zero-energy states for a given L increases. It is important that this nontrivial behavior is reproduced faithfully by the present method (see TABLE I).

Three electrons – Although unrecognized, the solution of the problem of three spin-polarized electrons in the LLL using molecular trial functions has been presented in Ref. [27]. Indeed, the wave functions in Jacobi coordinates in Eq. (18) of Ref. [27] are [8] precisely of the form

$\Phi_{3k}^{\text{REM}} Q_2^m$, as can be checked after transforming back to cartesian coordinates. It is noteworthy that Laughlin did not present molecular trial functions for electrons with $N > 3$, or for bosons for any N . This is done in the present paper.

Four electrons – For $N = 4$ spin-polarized electrons, one needs to consider two distinct molecular configurations, i.e., (0, 4) and (1, 3). Vibrations with $\lambda \geq 2$ must also be considered. In this case the RVM states are not always orthogonal, and the Gram-Schmidt orthogonalization is implemented.

Of particular interest is the $L = 18$ case ($\nu = 1/3$) which is considered [2] as the prototype of quantum-liquid states. However, in this case we found (see the Appendix) that the exact TI solutions are linear superpositions of the following seven RVM states [involving both the (0,4) and (1,3) configurations]: $|1\rangle = \Phi_{18}^{\text{REM}}(0, 4)$,

TABLE II: $N = 4$ LLL electrons with $L = 18$: Expansion coefficients in the RVM basis (labelled by the $|i\rangle$'s) for the three lowest-in-energy EXD-TI states (labelled [1], [2], [4]; see the Appendix). The 4th column gives the RVM expansion coefficients of the corresponding Jastrow-Laughlin expression.

RVM	EXD-TI [1]	EXD-TI [2]	EXD-TI [4]	JL
$ 1\rangle$	<u>0.9294</u>	-0.3430	0.0903	0.8403
$ 2\rangle$	-0.1188	-0.0693	<u>0.8930</u>	-0.1086
$ 3\rangle$	0.0067	0.0382	-0.2596	0.0076
$ 4\rangle$	0.0137	0.0191	-0.0968	0.0395
$ 5\rangle$	0.2540	<u>0.8486</u>	0.1519	0.4029
$ 6\rangle$	0.0211	0.0283	0.3097	0.0616
$ 7\rangle$	-0.2387	-0.3935	0.0877	-0.3380

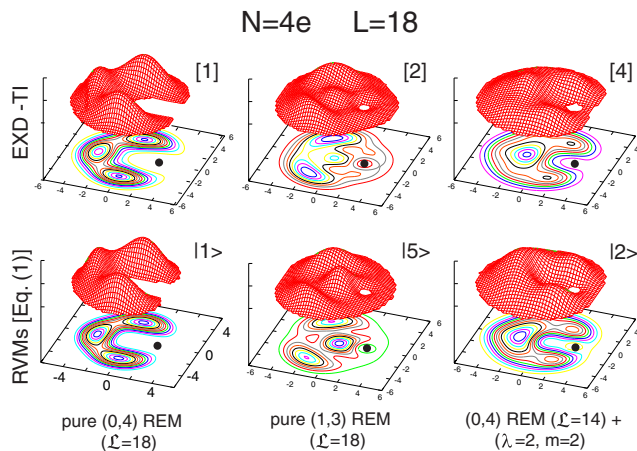


FIG. 1: CPDs for $N = 4$ LLL electrons with $L = 18$ ($\nu = 1/3$). Top row: The three lowest-in-energy EXD-TI states (see the Appendix). Bottom row: The RVM trial functions associated with the largest expansion coefficients (underlined, see TABLE II) of these three EXD-TI states in the correlated RVM basis. See the text for details. The solid dot denotes the fixed point \mathbf{r}_0 . Distances in nm.

$|2 \rangle = \Phi_{14}^{\text{REM}}(0, 4)Q_2^2$, $|3 \rangle = \Phi_{10}^{\text{REM}}(0, 4)Q_2^4$, $|4 \rangle = \Phi_6^{\text{REM}}(0, 4)Q_2^6$, $|5 \rangle = \Phi_{18}^{\text{REM}}(1, 3)$, $|6 \rangle = \Phi_{12}^{\text{REM}}(1, 3)Q_3^3$, and $|7 \rangle = \Phi_{15}^{\text{REM}}(1, 3)Q_3$. The expansion coefficients of the three lowest-in-energy EXD-TI states (labelled [1], [2], [4]; see the Appendix) in this RVM basis are listed in TABLE II. One sees that for each case, one component (underlined) dominates this expansion; this applies for both the yrast state (No. [1]) and the two excitations (Nos. [2] and [4]). To further illustrate this, we display in Fig. 1 the conditional probability (pair correlation) distributions (CPDs) $P(\mathbf{r}, \mathbf{r}_0)$ (see Eq. (1.1) in Ref. [9]) for these three EXD-TI states (top row) and for the RVM functions (bottom row) corresponding to the dominant expansion coefficients. The similarity of the CPDs in each column is noticeable and demonstrates that the single RVM functions capture the essence of many-body correlations in the EXD-TI states. Full quantitative agreement (within machine precision) in total energies can be reached by taking into consideration all seven RVM basis states (see the Appendix; also for other L 's, including $L = 30$ with 19 RVM basis states). Naturally, a smaller number of RVM states yields intermediate degrees of high-quality quantitative agreement.

The celebrated JL ansatz $\prod_{1 \leq i < j \leq N} (z_i - z_j)^{2p+1}$ has been given exclusively an interpretation of a quantum-fluid state [2, 7]. However, since the RVM functions span the TI subspace, it follows that any TI trial function (including the JL ansatz above and the compact CF states) can be expanded in the RVM basis. As an example, we give in TABLE II (4th column) the RVM expansion of the JL state for $N = 4e$ and $L = 18$. One sees that, compared to the EXD yrast state (1st column), the relative weight of the pure (0,4) REM (denoted by $|1 \rangle$) is re-

duced, while the weights of higher-in-energy vibrational excitations are enhanced. In this context, the liquid characteristics are due to the stronger weight of molecular vibrations which diminish the rigidity of the molecule.

Conclusions. – The many-body Hilbert space corresponding to the translationally invariant part of the LLL spectra of small systems (whether fermions or bosons, and for both low and high angular momenta) is spanned by the RVM trial functions introduced in Eq. (1). The yrast and excited states for both short- and long-range interactions can always be expressed as linear superpositions of these RVM functions. Thus the nature of strong correlations in the LLL reflects the emergence of intrinsic point-group symmetries associated with rotations and vibrations of molecules formed through particle localization. We stress the validity of the molecular theory for *low* angular momenta, where “quantum-liquid” physical pictures [2, 7, 19] have been thought to apply exclusively. Our analysis suggests that liquid-type pictures, associated with translationally invariant trial functions (e.g., the JL and compact CF functions), are reducible to a description in terms of an excited rotating/vibrating quantal molecule.

Work supported by the U.S. DOE (FG05-86ER45234).

APPENDIX

RBM analytic expression for $N = 4$ bosons – Here we present the case of $N = 4$ bosons having a (0, 4) one-ring molecular configuration. One has (within a normalization constant)

$$\Phi_{\mathcal{L}}^{\text{RBM}}(0, 4) = \sum_{\substack{l_1+l_2+l_3+l_4=\mathcal{L} \\ 0 \leq l_1 \leq l_2 \leq l_3 \leq l_4}} C(l_1, l_2, l_3, l_4) \text{Perm}[z_1^{l_1}, z_2^{l_2}, z_3^{l_3}, z_4^{l_4}], \quad (7)$$

where the symbol “Perm” denotes a permanent with elements $z_i^{l_j}$, $i, j = 1, 2, 3, 4$; only the diagonal elements are shown in Eq. (7). The coefficients were found to be:

$$C(l_1, l_2, l_3, l_4) = \left(\prod_{i=1}^4 l_i! \right)^{-1} \left(\prod_{k=1}^M p_k! \right)^{-1} \times \left(\sum_{n=1}^{4!} \mathcal{P}_n \cos \left[(3l_1 + l_2 - l_3 - 3l_4) \frac{\pi}{4} \right] \right), \quad (8)$$

where \mathcal{P}_n is an operator that generates the n th permutation of the boson labels (subscripts of l_i 's) 1, 2, 3, and 4. The index M (with $1 \leq M \leq 4$) denotes the number of different indices in the tetrad (l_1, l_2, l_3, l_4) and the p_k 's are the multiplicities of each one of the different indices.

TABLE III: LLL spectra of four spin-polarized electrons interacting via the Coulomb repulsion $e^2/(\kappa r_{ij})$. Second column: Dimensions of the full EXD and the nonspurious TI (in parenthesis) spaces (the EXD space is spanned by uncorrelated determinants of Darwin-Fock orbitals). Last three columns: Energy eigenvalues [in units of $e^2/(\kappa l_B)$] from the diagonalization of the Coulomb interaction in the TI subspace spanned by the trial functions $\Phi_{6+4k}^{\text{REM}}(0,4)Q_\lambda^m$ and $\Phi_{6+3k}^{\text{REM}}(1,3)Q_\lambda^m$ (RVM diagonalization). Third to sixth columns: the molecular configurations (n_1, n_2) and the quantum numbers k, λ and m are indicated within brackets. There is no nonspurious state with $L = 7$. The full EXD spectrum at a given L is constructed by including, in addition to the listed TI energy eigenvalues [$D^{\text{TI}}(L)$ in number], all the energies associated with angular momenta smaller than L . An integer in square brackets indicates the energy ordering in the full EXD spectrum (including both spurious and TI states), with [1] denoting an yrast state. Eight decimal digits are displayed, but the energy eigenvalues from the RVM diagonalization agree with the corresponding EXD-TI ones within machine precision.

L	$D^{\text{EXD}}(D^{\text{TI}})$	$[(n_1, n_2)\{k, \lambda, m\}]$	Energy eigenvalues (RVM diag. or EXD-TI)		
6	1(1)	[(0,4){0, λ ,0}]	2.22725097[1]		
8	2(1)	[(0,4){0,2,1}]	2.09240211[1]		
9	3(1)	[(1,3){1, λ ,0}]	1.93480798[1]		
10	5(2)	[(0,4){1, λ ,0}] [(0,4){0,2,2}]	1.78508849[1]	1.97809256[3]	
11	6(1)	[(1,3){1,2,1}]	1.86157215[2]		
12	9(3)	[(0,4){1,2,1}] [(0,4){0,2,3}] [(1,3){2, λ ,0}]	1.68518201[1]	1.76757420[2]	1.88068652[5]
13	11(2)	[(1,3){1,2,2}] [(0,4){1,3,1}]	1.64156849[1]	1.79962234[5]	
14	15(4)	[(0,4){2, λ ,0}] [(0,4){1,2,2}] [(0,4){0,2,4}]	1.50065835[1]	1.63572496[2]	1.72910626[5]
		[(1,3){2,2,1}]	1.79894008[8]		
15	18(3)	[(1,3){3, λ ,0}] [(1,3){2,3,1}] [(1,3){1,3,2}]	1.52704695[2]	1.62342533[3]	1.74810279[8]
18	34(7)	[(0,4){3, λ ,0}] [(0,4){2,2,2}] [(0,4){1,2,4}]	1.30572905[1]	1.41507954[2]	1.43427543[4]
		[(0,4){0,2,6}] [(1,3){4, λ ,0}] [(1,3){2,2,3}]	1.50366728[8]	1.56527615[11]	1.63564655[15]
		[(1,3){3,3,1}]	1.68994048[20]		

For example, for (2,2,2,5), one has $M = 2$ and $p_1 = 3$, $p_2 = 1$; for (0,0,0,0), one has $M = 1$ and $p_1 = 4$; for (1,2,3,9), one has $M = 4$ and $p_1 = p_2 = p_3 = p_4 = 1$.

Expressions for any number N of bosons and any molecular configuration (n_1, n_2, \dots, n_q) can also be derived and will be presented in a future publication [28].

LLL spectrum of four polarized electrons – For $N = 4$ spin-polarized electrons, one needs to consider rovibrational states [see Eq. (1) in the main text] for two distinct molecular configurations, i.e., $\Phi_{6+4k}^{\text{REM}}(0,4)Q_\lambda^m$ and $\Phi_{6+3k}^{\text{REM}}(1,3)Q_\lambda^m$. TABLE III summarizes the quantal molecular description in the start of the LLL spectrum ($6 \leq L \leq 15$ and $L = 18$).

In several cases the nonspurious (TI) states are given by a single trial function as defined in Eq. (1) of the main text. Indeed for $L = 9$ the yrast state is a pure REM state, i.e., $\Phi_9^{\text{REM}}(1,3)$. For $L = 11$ the single nonspurious state is the first excited state in the full spectrum, coinciding with the molecular vibration $\Phi_9^{\text{REM}}(1,3)Q_2$.

Of particular interest is the $L = 18$ case; it corresponds to the celebrated $\nu = 1/3$ fractional filling, which is considered [2] as the prototype of quantum liquid states. However, in this case we found (see TABLE III) that the EXD-TI nonspurious solutions are linear superpositions of seven molecular states involving dipole ($\lambda = 2$) and octupole ($\lambda = 3$) vibrations relative to both the (0,4) and (1,3) configurations. Focusing on the yrast state with $L = 18$, we found that its largest component is the pure $\Phi_{18}^{\text{REM}}(0,4)$ REM state with a 0.9294 overlap with the EXD solution (see TABLE II in the main text); the contributions of the remaining six states are much

smaller, but they bring the overlap to precisely unity. Unlike the $\nu = 1/2$ case of bosons, we stress that the fermionic Jastrow-Laughlin functions at all ν 's exhibit less-than-unity overlaps [2, 7].

Of great interest also is the $L = 30$ ($\nu = 1/5$) case, which in the composite-fermion picture was found to be susceptible to a competition [29] between crystalline and liquid orders. However, we found that the exact nonspurious states for $L = 30$ are actually linear superpositions of the following 19 [= $D^{\text{TI}}(L = 30)$] RVM functions: $\Phi_{6+4k}^{\text{REM}}(0,4)Q_2^{12-2k}$, with $k = 0, 1, 2, 3, 4, 5, 6$; $\Phi_{6+3k}^{\text{REM}}(1,3)Q_2^{12-3k/2}$, with $k = 2, 4, 6$; $\Phi_{6+4k}^{\text{REM}}(0,4)Q_3^{8-4k/3}$, with $k = 0, 3$; and $\Phi_{6+3k}^{\text{REM}}(1,3)Q_3^{8-k}$, with $k = 2, 3, 4, 5, 6, 7, 8$. Diagonalization of the Coulomb interaction in the above TI subspace yielded an energy 0.25084902 $e^2/(\kappa l_B)$ per electron for the yrast state; this value agrees again, within machine precision, with the EXD result. The most sophisticated variants of the composite-fermion theory [including composite-fermion diagonalization (CFD), composite-fermion crystal (CFC), and mixed liquid-CFC states [7, 10, 29]] fall short in this respect. Indeed the following higher energies were found [29, 30]: 0.250863(6) (CFD), 0.25094(4) (mixed), 0.25101(4) (CFC). The CFD basis is not translationally invariant [10]. Consequently, to achieve machine-precision accuracy, the CFD will have to be performed in the larger space of dimension $D^{\text{EXD}}(L = 30) = 169$.

-
- [1] D.C. Tsui *et al.*, Phys. Rev. Lett. **48**, 1559 (1982).
- [2] R.B. Laughlin, Phys. Rev. Lett. **50**, 1395 (1983); Rev. Mod. Phys. **71**, 863 (1999), and references therein.
- [3] S.A. Trugman and S. Kivelson, Phys. Rev. B **31**, 5280 (1985).
- [4] G. Moore and N. Read, Nucl. Phys. B **360**, 362 (1991).
- [5] M. Stone *et al.*, Phys. Rev. B **45**, 14 156 (1992).
- [6] J.H. Oaknin *et al.*, Phys. Rev. Lett. **74**, 5120 (1995).
- [7] J.K. Jain, *Composite Fermions* (Cambridge University Press, 2007), and references therein.
- [8] C. Yannouleas and U. Landman, Phys. Rev. B **66**, 115315 (2002).
- [9] C. Yannouleas and U. Landman, Rep. Prog. Phys. **70**, 2067 (2007), and references therein.
- [10] G.S. Jeon *et al.*, Phys. Rev. B **69**, 241304(R) (2004); Eur. Phys. J. B **55**, 271 (2007).
- [11] B.R. Mottelson, Phys. Rev. Lett. **83**, 2695 (1999).
- [12] K. Wilkin and J.M.F. Gunn, Phys. Rev. Lett. **84**, 6 (2000).
- [13] Th. Papenbrock and G.F. Bertsch, Phys. Rev. A **63**, 023616 (2001).
- [14] M. Ueda and T. Nakajima, Phys. Rev. A **64**, 063609 (2001).
- [15] M. Popp *et al.*, Phys. Rev. A **70**, 053612 (2004).
- [16] N. Barberán *et al.*, Phys. Rev. A **73**, 063623 (2006).
- [17] L.O. Baksmaty *et al.*, Phys. Rev. A **75**, 023620 (2007).
- [18] S. Viefers, J. Phys.: Condens. Matter **20**, 123202 (2008).
- [19] N.R. Cooper, Adv. Phys. **57**, 539 (2008), and references therein.
- [20] N.D. Gemelke, Ph.D. Dissertation (Stanford University, 2007); Steven Chu, Book of Abstracts, ICAP 2008, p. 5.
- [21] S.K. Baur *et al.*, Phys. Rev. A **78**, 061608 (2008).
- [22] M.I. Parke *et al.*, Phys. Rev. Lett. **101**, 110401 (2008).
- [23] An yrast state has the lowest energy at a given L .
- [24] *Classical* approaches have also been used for constructing molecular models of the LLL spectrum (lower part). They perform better at high L (with $\nu < 1/9$); see P.A. Maksym, Phys. Rev. B **53** 10 871 (1996), and J.-P. Nikkarila *et al.*, Sol. State Commun. **141**, 209 (2007).
- [25] Ref. [3] multiplied the elementary symmetric polynomials by a Pauli-exclusion single-determinant factor to generate a basis spanning the fermionic TI subspace, but which has no physical picture associated with it.
- [26] R.A. Smith and N.K. Wilkin, Phys. Rev. A **62**, 061602(R) (2000).
- [27] R.B. Laughlin, Phys. Rev. B **27**, 3383 (1983).
- [28] C. Yannouleas, in preparation.
- [29] C.C. Chang *et al.*, Phys. Rev. B **73**, 155323 (2006).
- [30] Numbers shown in parentheses are statistical uncertainties arising from Monte Carlo sampling.